

Highly anisotropic and electric field tunable Zeeman splittings in Mn-doped CdS nanowires

Xiu-Wen Zhang,^{1,2} Wei-Jun Fan,¹ Shu-Shen Li,² and Jian-Bai Xia²

¹*School of Electrical and Electronic Engineering, Nanyang Technological University, Singapore 639798, Singapore*

²*State Key Laboratory for Superlattices and Microstructures, Institute of Semiconductors, Chinese Academy of Sciences, P.O. Box 912, Beijing 100083, China*

(Received 27 June 2007; revised manuscript received 28 August 2007; published 8 November 2007)

The electronic structure, Zeeman splitting, and g factor of Mn-doped CdS nanowires are studied using the $k \cdot p$ method and the mean field model. It is found that the Zeeman splittings of the hole ground states can be highly anisotropic, and so can their g factors. The hole ground states vary a lot with the radius. For thin wire, g_z (g factor when B is along the z direction or the wire direction) is a little smaller than g_x . For thick wire, g_z is much larger than g_x at small magnetic field, and the anisotropic factor g_z/g_x decreases as B increases. A small transverse electric field can change the Zeeman splitting dramatically, so tune the g_x from nearly 0 to 70, in thick wire. The anisotropic factor decreases rapidly as the electric field increases. On the other hand, the Zeeman splittings of the electron ground states are always isotropic.

DOI: 10.1103/PhysRevB.76.195306

PACS number(s): 73.21.Hb, 75.75.+a, 75.90.+w

I. INTRODUCTION

Nowadays, much of the research in semiconductor physics has been shifting toward diluted magnetic semiconductors (DMSs),¹⁻³ which have extensive applications in spin-dependent quantum computing devices that combine logic and storage functions. Manganese-doped II-VI (Refs. 4 and 5) and III-V (Ref. 1) compound semiconductors have been widely studied. Transportation⁶ and manipulation⁷ of carriers' spin in DMSs were experimentally reported.

Meanwhile, the investigations of quantum confinement of carriers in spatially modulated semiconductor structures have been a field of intense activity over the past decades. High-quality CdS nanowires were synthesized and used as photonic circuit elements.⁸⁻¹¹ The electronic structure of semiconductor nanowires was studied using the $k \cdot p$ method.^{12,13} The method to dope Mn ions into CdS nanowires was achieved.¹⁴⁻¹⁶ The electronic, optical, and transport properties of DMS nanowires were investigated extensively.¹⁴⁻¹⁸ Recently, the electronic structure and Zeeman splitting of paramagnetic Mn-doped ZnO nanowires were theoretically studied.¹⁹

The anisotropic Zeeman splitting was earlier found in the GaAs/AlAs quantum wells.²⁰ The fine structure of excitons in GaAs/AlAs quantum wells showed that the perpendicular (to the well plane) g factors of the heavy hole g_{hz} are in between 2 and 3, while the in-plane values g_{hx} and g_{hy} are smaller than 0.01. This strong anisotropy of the effective hole g value is a consequence of description of the heavy-hole states with $J_{hz} = \pm \frac{3}{2}$ by an effective spin $S_h = \frac{1}{2}$. From the spin Hamiltonian, it can be seen that the in-plane splittings can only be due to the cubic hole Zeeman interaction terms. The small values of g_{hx} and g_{hy} correspond to a small q value in a bulk semiconductor. On the other hand, the bulk linear hole Zeeman splitting constant κ , which is about 1.2 for GaAs, results in a large g_{hz} value for GaAs layer samples.

Recently, the anisotropic Zeeman splitting has been found in ballistic one-dimensional hole systems.^{21,22} The splitting of the subband edges is shown in the transconductance grayscale plot when an in-plane magnetic field is applied parallel

to the one-dimensional (1D) GaAs hole systems. In contrast, the transconductance grayscale shows that the degenerate 1D subbands are not affected by the perpendicular magnetic field up to 8.8 T; i.e., no Zeeman splitting is seen when the magnetic field is aligned perpendicular to the channel. This anisotropy of the effective g factor is a direct consequence of the one-dimensional confinement on a system with strong spin-orbit coupling. We will study how the spin-orbit coupling and the quantum confinement will affect the Zeeman splitting in wurtzite $\text{Cd}_{1-x}\text{Mn}_x\text{S}$ nanowires.

In this paper, we use the effective-mass model of semiconductor nanowires, taking into account the $sp-d$ exchange interaction, for the study of the electronic structure, Zeeman splitting, and especially, the anisotropic g factor of hole states in paramagnetic Mn-doped CdS nanowires under magnetic and electric fields. The remainder of this paper is organized as follows. The calculation model is given in Sec. II, the results and discussion are given in Sec. III, and Sec. IV is the conclusion.

II. THEORETICAL MODEL AND CALCULATIONS

In the absence of external fields, we represent the six-band effective-mass Hamiltonian of the hole in the basis functions $|11\rangle\uparrow$, $|10\rangle\uparrow$, $|1-1\rangle\uparrow$, $|11\rangle\downarrow$, $|10\rangle\downarrow$, and $|1-1\rangle\downarrow$ as

$$H_{h0} = \begin{pmatrix} H_{int} & \\ & H_{int} \end{pmatrix} + H_{so}. \quad (1)$$

Here, H_{so} is the valence band spin-orbit coupling Hamiltonian which was given before,¹² and the spin-orbit splitting energy of CdS is $\Delta_{so} = 70$ meV. H_{int} is written as

$$H_{int} = -\frac{1}{2m_0} \begin{pmatrix} P_1 & S & T \\ S^* & P_3 & S \\ T^* & S^* & P_1 \end{pmatrix}, \quad (2)$$

where

$$P_1 = \frac{L+M}{2} p_- p_+ + N p_z^2, \quad (3a)$$

$$P_3 = Sp_{-p_+} + Tp_z^2 + 2m_0\Delta_c, \quad (3b)$$

$$T = \frac{L-M-R}{4}p_+^2 + \frac{L-M+R}{4}p_-^2, \quad (3c)$$

$$T^* = \frac{L-M-R}{4}p_-^2 + \frac{L-M+R}{4}p_+^2, \quad (3d)$$

$$S = \frac{1}{\sqrt{2}}Qp_{-p_z}, \quad (3e)$$

$$S^* = \frac{1}{\sqrt{2}}Qp_{+p_z}, \quad (3f)$$

$$p_{\pm} = p_x \pm ip_y. \quad (3g)$$

Here, L, M, \dots, Q are the effective-mass parameters and Δ_c is the crystal field splitting energy, which were given before.¹²

The effective-mass Hamiltonian of the electron in the absence of external fields is

$$H_{e0} = \frac{1}{2m_x^*}p_{-p_+} + \frac{1}{2m_z^*}p_z^2 + E_g, \quad (4)$$

where $m_x^* = 0.1806m_0$, $m_z^* = 0.1788m_0$ are the electron effective masses and $E_g = 2.582$ eV is the band gap.²³

We assume that the electric field is applied along the x direction. The electric field potential term is written as

$$V = e\mathbf{F} \cdot \mathbf{r} = eFx = eFr \cos \theta = \frac{1}{2}eFre^{i\theta} + \frac{1}{2}eFre^{-i\theta}. \quad (5)$$

We choose the magnetic field along the x or z direction. In the absence of magnetic ions, the magnetic field introduces three terms in the hole Hamiltonian, the antisymmetric term H_{asym} , the magnetic-momentum term H_{mm} , and the spin-Zeeman-splitting term $H_{Zeeman,h}$,²⁴ and it also introduces the spin-Zeeman-splitting term $H_{Zeeman,e}$ in the electron Hamiltonian. In the presence of magnetic ions, the magnetic field brings the magnetization of the localized spins, so it introduces two other terms, the s - d and p - d exchange interaction terms between the carriers and the magnetic ion, H_{sd} and H_{pd} in the electron and hole Hamiltonians, respectively. They are written as³

$$H_{sd} = \alpha s_e \cdot \mathbf{M} / (g_{Mn} \mu_B), \quad (6)$$

$$H_{pd} = \beta s_h \cdot \mathbf{M} / (g_{Mn} \mu_B), \quad (7)$$

where $g_{Mn} = 2$ is the g factor of magnetic ion, $s_e(s_h)$ is the spin ($s_e = s_h = \frac{1}{2}$) of electron (hole), αN_0 and βN_0 are the s - d and p - d exchange constants, and N_0 is the number of cations per unit volume. For Mn-doped CdS, $\alpha N_0 = 0.22$ eV and $\beta N_0 = -1.8$ eV.²⁵ \mathbf{M} is the magnetization of the localized spins of the magnetic ions. In the paramagnetic case, \mathbf{M} is parallel to the external magnetic field, the magnitude of \mathbf{M} is given by³

$$M = S g_{Mn} \mu_B N_0 x_{eff} B_S \left[\frac{S g_{Mn} \mu_B B}{k_B (T + T_{AF})} \right], \quad (8)$$

where $S = \frac{5}{2}$ is the spin of magnetic ion, x_{eff} is the effective content of magnetic ions, T_{AF} accounts for the reduced single-ion contribution due to the antiferromagnetic Mn-Mn coupling, and the Brillouin function $B_S(x)$ is

$$B_S(x) = \frac{2S+1}{2S} \coth\left(\frac{2S+1}{2S}x\right) - \frac{1}{2S} \coth\left(\frac{1}{2S}x\right). \quad (9)$$

For Mn-doped CdS, $T_{AF} = 1$ K.³ The total hole and electron Hamiltonians in the presence of electric and magnetic fields are written as

$$H_h = H_{h0} + V + H_{asym} + H_{mm,h} + H_{Zeeman,h} + H_{pd}, \quad (10)$$

$$H_e = H_{e0} + V + H_{mm,e} + H_{Zeeman,e} + H_{sd}. \quad (11)$$

We assume that the nanowires have cylindrical symmetry, the longitudinal axis is along the z direction, and the electrons and holes are confined laterally in an infinitely high potential barrier. The longitudinal wave function is the plane wave, and the lateral wave function is expanded in Bessel functions. The hole and electron envelope functions are

$$\Psi_{k_z}^h = \sum_J \sum_n \begin{pmatrix} b_{l-1,n,\uparrow} A_{l-1,n} J_{l-1}(k_n^{l-1} r) e^{i(l-1)\theta} \\ c_{l,n,\uparrow} A_{l,n} J_l(k_n^l r) e^{i\theta} \\ d_{l+1,n,\uparrow} A_{l+1,n} J_{l+1}(k_n^{l+1} r) e^{i(l+1)\theta} \\ b_{l,n,\downarrow} A_{l,n} J_l(k_n^l r) e^{i\theta} \\ c_{l+1,n,\downarrow} A_{l+1,n} J_{l+1}(k_n^{l+1} r) e^{i(l+1)\theta} \\ d_{l+2,n,\downarrow} A_{l+2,n} J_{l+2}(k_n^{l+2} r) e^{i(l+2)\theta} \end{pmatrix} e^{ik_z z}, \quad (12)$$

$$\Psi_{k_z}^e = \sum_l \sum_n \begin{pmatrix} e_{l,n,\uparrow} A_{l,n} J_l(k_n^l r) e^{i\theta} \\ e_{l,n,\downarrow} A_{l,n} J_l(k_n^l r) e^{i\theta} \end{pmatrix} e^{ik_z z}, \quad (13)$$

respectively, where $J = l + 1/2$ and $A_{l,n}$ is the normalization constant,

$$A_{l,n} = \frac{1}{\sqrt{\pi R} J_{l+1}(\alpha_n^l)}. \quad (14)$$

Here, $\alpha_n^l = k_n^l R$ is the n th zero point of $J_l(x)$, R is the radius of the wire, and k_z is the wave vector along the wire direction, which is a good quantum number.

III. RESULTS AND DISCUSSION

In this section, we calculate the electronic structure, Zeeman splitting, and g factor of the Mn-doped CdS nanowires under magnetic and electric fields using the $k \cdot p$ method and the mean field model.

Figures 1(a) and 1(b) show the electron and hole energy levels of Mn-doped CdS nanowires as functions of the radius R at $k_z = 0$, $B = 0$, and $F = 0$. The main state components of some levels are labeled; for example, $(1,0)X^{\uparrow}$ means that the state has the envelope function with $n = 1$, $l = 0$ [see Eqs.

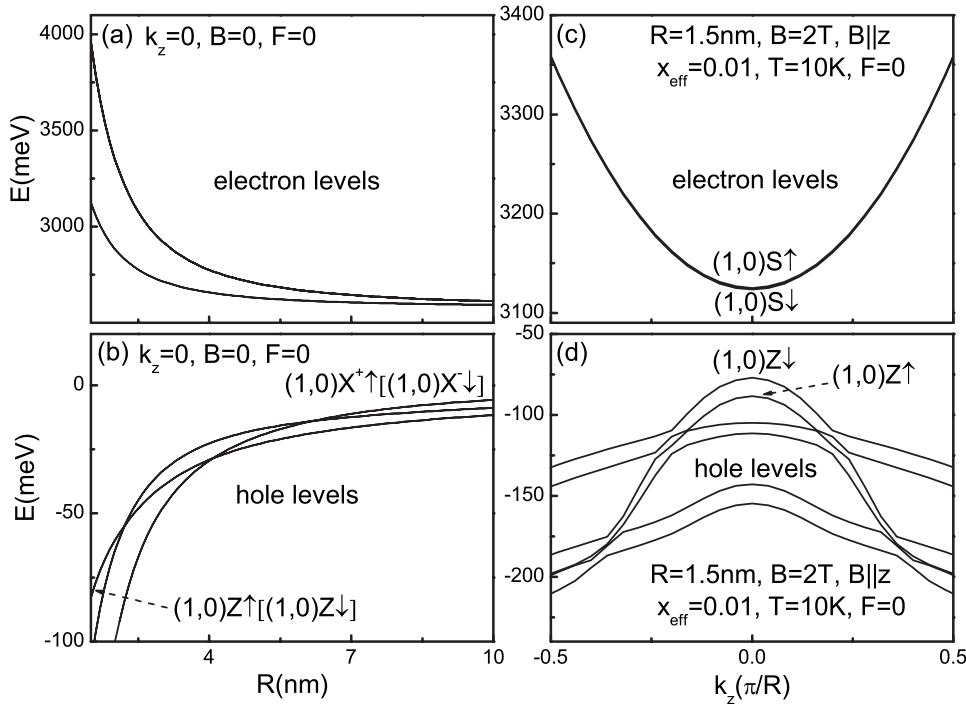


FIG. 1. Energy levels of Mn-doped CdS nanowires in the absence of electric field. (a) Electron levels as functions of R at $B=0$ and $k_z=0$. (b) Hole levels similar to (a). (c) Electron levels as functions of k_z for $R=1.5$ nm, $B=2$ T ($B\parallel z$), $x_{eff}=0.01$, and $T=10$ K. (d) Hole levels similar to (c).

(12) and (13)], the Bloch function [11], and the spin-up state. The electron levels decrease and hole levels increase as R increases. When $R < 2$ nm, the hole ground states have the components $(1,0)Z\uparrow$ and $(1,0)Z\downarrow$, while when $R > 7$ nm, they have the components $(1,0)X^+\uparrow$ and $(1,0)X^-\downarrow$. Thus, the hole ground states vary a lot with R . Figures 1(c) and 1(d) show the electron and hole energy levels of Mn-doped CdS nanowires with $R=1.5$ nm as functions of the wave vector k_z

at $B=2$ T ($B\parallel z$), $x_{eff}=0.01$, $T=10$ K, and $F=0$. From the figures, we see that the energy levels split greatly at $B=2$ T due to their $sp-d$ exchange interaction with the Mn ion [see Eqs. (6) and (7)].

Figures 2(a) and 2(b) show the electron energy levels of Mn-doped CdS nanowires with $R=1.5$ nm as functions of B at $x_{eff}=0.01$, $T=10$ K, $k_z=0$, and $F=0$ in the cases of $B\parallel z$ and $B\parallel x$, respectively. Figures 2(c) and 2(d) are the same but

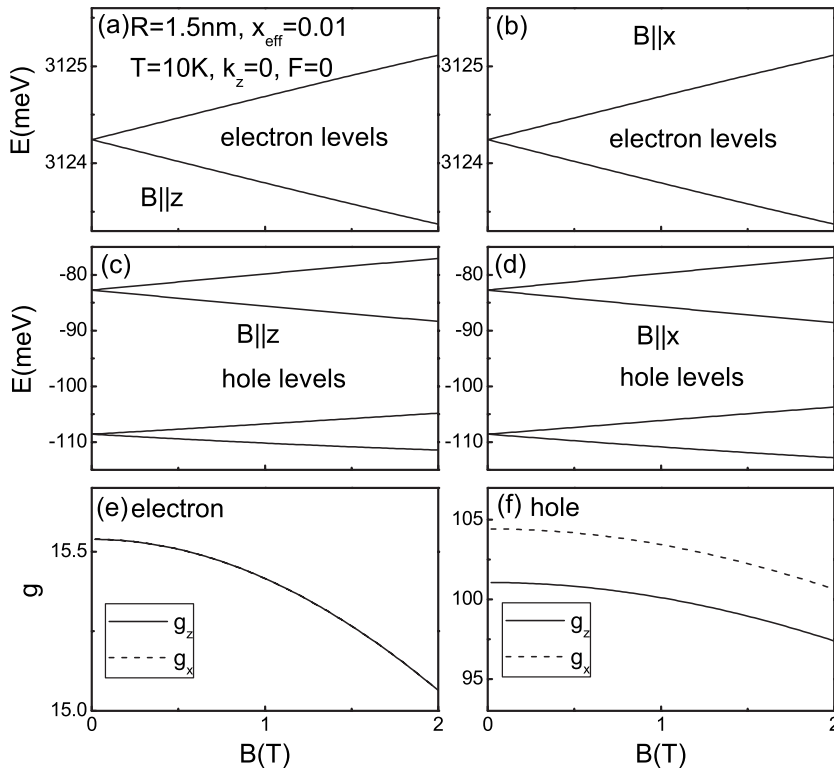


FIG. 2. Energy levels and g factors of Mn-doped CdS nanowires with $R=1.5$ nm and $x_{eff}=0.01$ at $T=10$ K, $k_z=0$, and $F=0$ as functions of B . (a) Electron levels $B\parallel z$. (b) Electron levels $B\parallel x$. (c) Hole levels $B\parallel z$. (d) Hole levels $B\parallel x$. (e) Electron g factors. (f) Hole g factors.

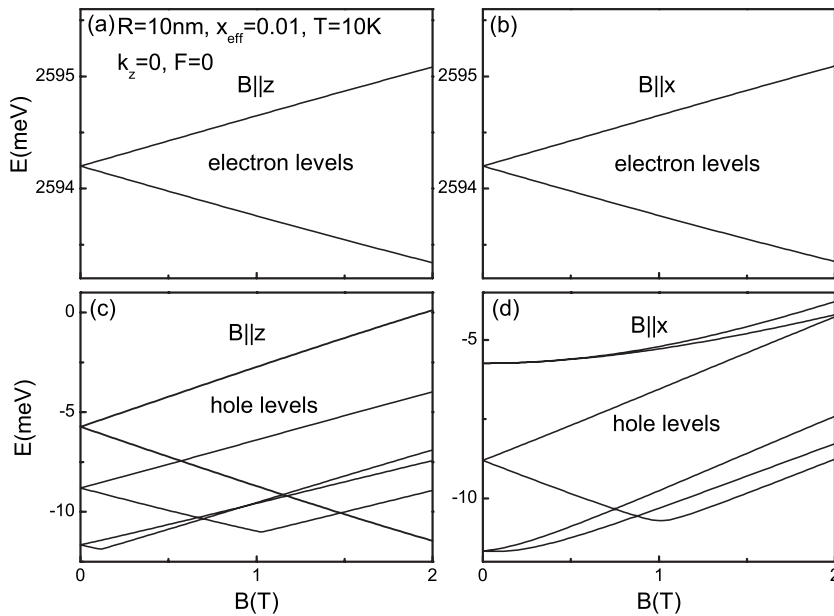


FIG. 3. Energy levels of Mn-doped CdS nanowires with $R = 10$ nm and $x_{eff} = 0.01$ at $T = 10$ K, $k_z = 0$, and $F = 0$ as functions of B . (a) Electron levels $B \parallel z$. (b) Electron levels $B \parallel x$. (c) Hole levels $B \parallel z$. (d) Hole levels $B \parallel x$.

for the hole energy levels. The Zeeman splittings are similar for different magnetic field directions; i.e., they are almost isotropic. The splitting energy ΔE increases nearly linearly with B , then shows a saturation trend when B is large, which is not clear in the figures. We can define a g factor $g = \Delta E / (\mu_B B)$ to denote the Zeeman splitting energy at a given magnetic field. The g_z and g_x factors of the electron and hole ground states as functions of B for $R = 1.5$ nm wire are shown in Figs. 2(e) and 2(f), respectively. g_z (g_x) is the g factor when the magnetic field is along the z (x) direction. We note that the g factor decreases as B increases, which indicates the saturation trend of the Zeeman splittings. It is due to the saturation of the magnetization of the localized spins as B increases [see Eq. (8)]. For the electron ground states, $g_z = g_x$, i.e., they are exactly isotropic. While for the hole ground states, g_z is a little smaller than g_x , so they are a little anisotropic.

Figures 3(a) and 3(b) show the electron energy levels of Mn-doped CdS nanowires with $R = 10$ nm as functions of B at $x_{eff} = 0.01$, $T = 10$ K, $k_z = 0$, and $F = 0$ in the cases of $B \parallel z$ and $B \parallel x$, respectively. Figures 3(c) and 3(d) are the same but for the hole energy levels. The Zeeman splittings of electron ground states are still isotropic. We see from Fig. 3(d) that when $B \parallel x$, the Zeeman splitting of hole ground states is very small, while the Zeeman splitting when $B \parallel z$ [Fig. 3(c)] is large. Thus, the Zeeman splittings of the hole ground states are highly anisotropic, and g_z is very larger than g_x . Figures 4(a) and 4(b) show the g_z and g_x factors of the ground states as functions of B for electron and hole, respectively. We see from Figs. 4(a) and 4(b) that for electron states, g_z is nearly the same as g_x , decreasing with increasing B which is similar to the cases in Figs. 2(e) and 2(f), but for hole states, g_x is much smaller than g_z . The g_x increases slightly as B increases because the second excited states split normally and

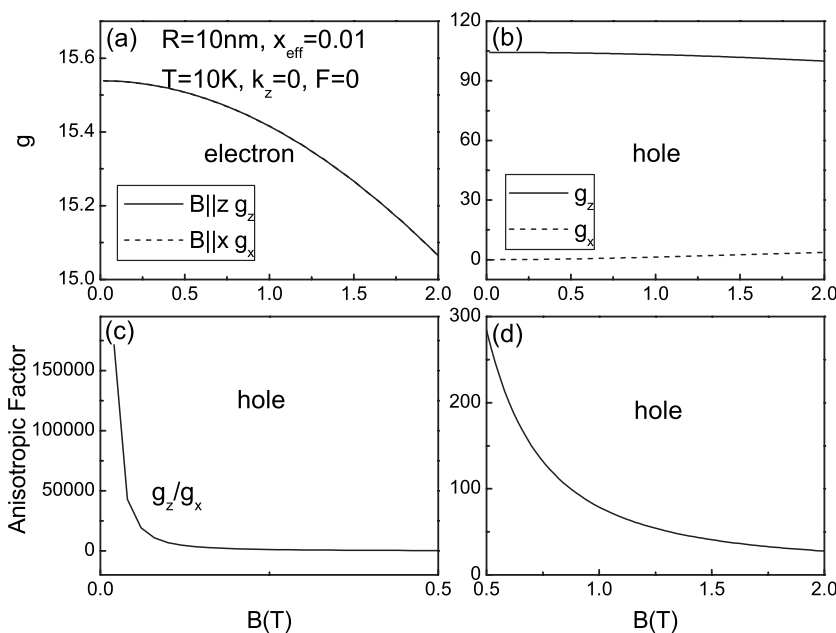


FIG. 4. g factors and their anisotropic factor of Mn-doped CdS nanowires with $R = 10$ nm and $x_{eff} = 0.01$ at $T = 10$ K, $k_z = 0$, and $F = 0$ as functions of B . (a) Electron g factors. (b) Hole g factors. [(c) and (d)] The anisotropic factor of hole g factors.

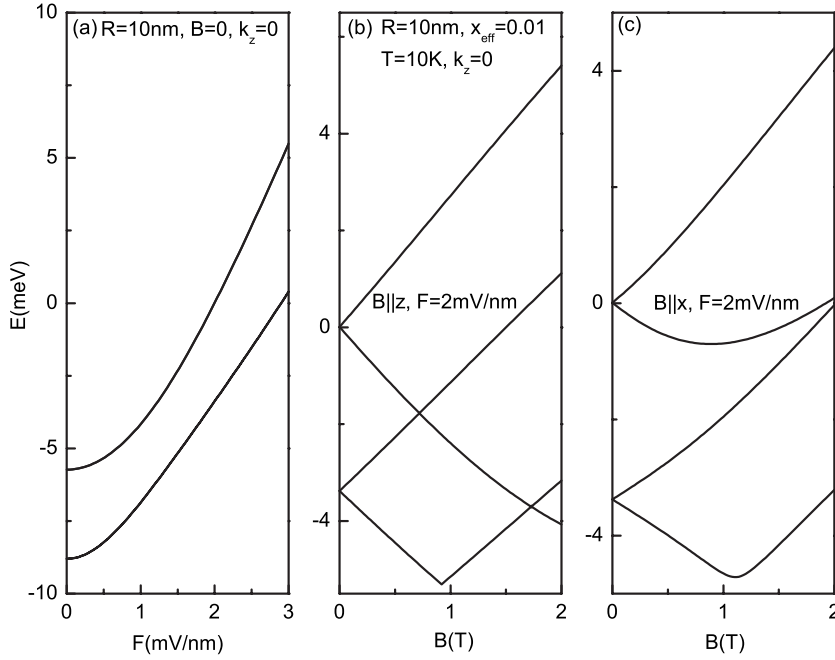


FIG. 5. Hole levels of Mn-doped CdS nanowires with $R = 10$ nm and $x_{eff} = 0.01$ at $T = 10$ K and $k_z = 0$. (a) $B = 0$ as functions of F . (b) $F = 2$ mV/nm as functions of B ($B \parallel z$). (c) $F = 2$ mV/nm as functions of B ($B \parallel x$).

one of them becomes close to the hole ground states and couples with them, leading to their splitting. In order to denote the anisotropy, we define an anisotropic factor of the Zeeman splitting for the hole ground states as g_z/g_x , which is shown in Figs. 4(c) and 4(d) as functions of B in the range of $0 < B < 0.5$ T and $0.5 < B < 2$ T, respectively. We see that the anisotropic factor can be as large as 170 000 at small magnetic field, and decreases when B increases because g_z decreases and g_x increases. The highly anisotropic Zeeman splitting of nanowires will lead to highly anisotropic magnetotransport for different magnetic field directions. This anisotropic magnetotransport effect is significant at low temperature, while it is tiny when the temperature is very high due to the carriers' thermal distribution. The highly anisotropic Zeeman splitting of hole ground states appears in thick nanowires while disappears in thin nanowires because there are two level crossings of the highest hole levels and the hole ground states vary with the radius [see Fig. 1].

Physically, the highly anisotropic Zeeman splitting is induced by the spin-orbit coupling effect, which makes the spin states couple with the space-wave functions. The space-wave functions are anisotropic due to the crystal field splitting energy (Δ_c) and the anisotropic shape of the wire (from the z direction to x direction). This makes the spin states anisotropic. The spin-orbit coupling in the conduction band of CdS is neglectable, so the spin states of the electron states are isotropic. We see that the electron ground states $(1,0)S \uparrow$ and $(1,0)S \downarrow$ have the same space-wave function $(1,0)S$. There are some hole states whose spin states are basically isotropic, for example, the hole ground states of $R = 1.5$ nm wire $(1,0)Z \uparrow$ and $(1,0)Z \downarrow$ which have the same space-wave function $(1,0)Z$. While some hole states have highly anisotropic spin states, for example, the hole ground states of $R = 10$ nm wire $(1,0)X^+ \uparrow$ and $(1,0)X^- \downarrow$ whose space-wave functions $(1,0)X^+$ and $(1,0)X^-$ are quite different. In the hole Hamiltonian [Eq. (10)], there are three terms which induce

Zeeman splitting: the H_{asym} , $H_{Zeeman,h}$, and H_{pd} ; the last one dominates when x_{eff} is not too small. When $B \parallel z$, the three terms can be written as $A\sigma_z$, BI_z ,²⁴ and $C\sigma_z$, respectively; A , B , and C are the coefficients. They have large matrix elements in the states of $(1,0)X^+ \uparrow$ and $(1,0)X^- \downarrow$, leading to large Zeeman splitting. When $B \parallel x$, the three terms can be written as $A\sigma_x$, BI_x , and $C\sigma_x$, respectively. $A\sigma_x$ and $C\sigma_x$ have zero matrix elements between the states of $(1,0)X^+ \uparrow$ and $(1,0)X^- \downarrow$ as their space-wave functions are orthogonal. BI_x has zero matrix element between the states of $(1,0)X^+ \uparrow$ and $(1,0)X^- \downarrow$ because the spin states are orthogonal. That is why the Zeeman splitting in Fig. 3(d) is tiny in the case of $B \parallel x$. While for the states whose space-wave functions are same, such as $(1,0)Z \uparrow$ and $(1,0)Z \downarrow$, the Zeeman terms have large matrix elements in both the cases of $B \parallel z$ and $B \parallel x$. Therefore, the states which have very different space-wave functions have highly anisotropic Zeeman splitting. The former works on highly anisotropic Zeeman splittings²⁰⁻²² focused on the heavy-hole states whose space-wave functions are different [such as $(1,0)X^+ \uparrow$ and $(1,0)X^- \downarrow$ in Fig. 1]. Our result can be used to explain the former experimental results²⁰⁻²² and suggests to investigate the highly anisotropic Zeeman splitting of other states that have very different space-wave functions.

Figure 5(a) shows the hole energy levels of Mn-doped CdS nanowires with $R = 10$ nm as functions of the transverse electric field F at $B = 0$ and $k_z = 0$. We see that an external electric field can make the hole states coupled with each other, resulting in the mixing of the wave functions and the energy levels anticrossing. The coupling of states will change the Zeeman splitting dramatically. Figures 5(b) and 5(c) show the hole energy levels of Mn-doped CdS nanowires with $R = 10$ nm as functions of B at $x_{eff} = 0.01$, $T = 10$ K, $k_z = 0$, and $F = 2$ mV/nm in the cases of $B \parallel z$ and $B \parallel x$, respectively. We find that the Zeeman splitting in the $B \parallel x$ case is large even B is small, which is contrary to that when $F = 0$ [see Fig. 3(d)]. It is due to the mixing of the nearly isotropic

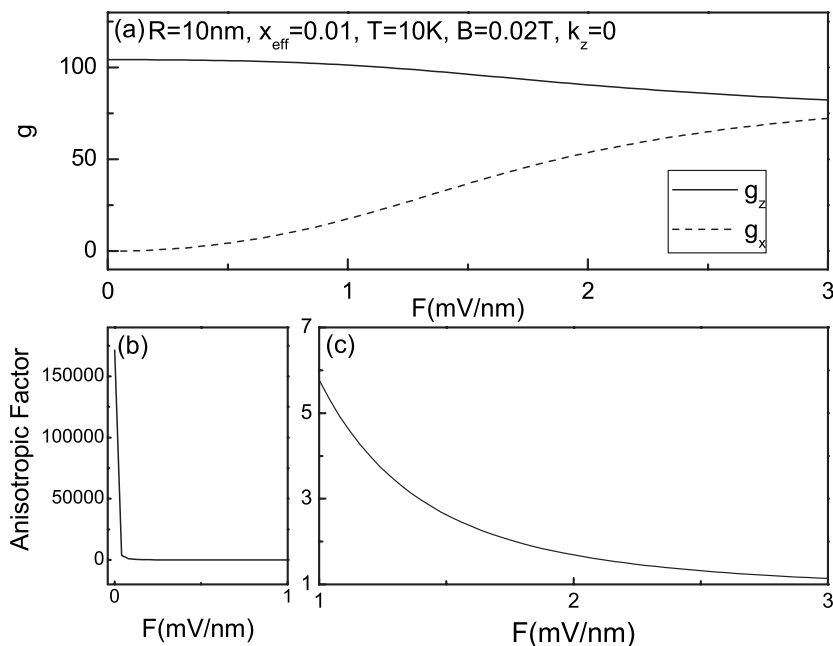


FIG. 6. Hole g factors and their anisotropic factor of Mn-doped CdS nanowires with $R = 10$ nm and $x_{eff} = 0.01$ at $T = 10$ K, $B = 0.02$ T, and $k_z = 0$ as functions of F . (a) Hole g factors. [(b) and (c)] The anisotropic factor of hole g factors.

components into the originally anisotropic hole ground states $(1,0)X^+\uparrow$ and $(1,0)X^-\downarrow$. The Zeeman splitting in the $B\parallel z$ case is affected a little by the electric field. Figure 6(a) shows the g_z and g_x factors of the hole ground states in $R = 10$ nm wire as functions of F at $x_{eff} = 0.01$, $T = 10$ K, $k_z = 0$, and $B = 2$ T. It is interesting to note that the g_z decreases as F increases, and the g_x increases from nearly 0 to 70 when the electric field increases from 0 to just 3 mV/nm which is comparatively small. Figures 6(b) and 6(c) show the anisotropic factor (g_z/g_x) as functions of F for the range $0 < F < 1$ mV/nm and $1 < F < 3$ mV/nm, respectively. We see that the g_z/g_x decreases from 170 000 to nearly 1 rapidly as the electric field increases. So a small electric field can tune the g factor dramatically. As DMS nanowires can be used for spin-dependent transportation,¹⁷ by using the Zeeman splitting of the ground states, a small external electric field can be used to control the spin-dependent transportation in DMS nanowires.

IV. CONCLUSIONS

In summary, the electronic structure, Zeeman splitting, and g factor of Mn-doped CdS nanowires were studied using

the $k \cdot p$ method and the mean field model. It was found that the Zeeman splittings of the hole ground states are anisotropic for different magnetic field (B) directions, and so are their g factors, due to the spin-orbit coupling effect. The hole ground states vary a lot with the radius. For thin wire, g_z is a little smaller than g_x . For thick wire, g_z is 170 000 times larger than g_x at small magnetic field, and the anisotropic factor g_z/g_x decreases as B increases. A small transverse electric field can change the Zeeman splitting of the hole ground states dramatically, so tune the g_x from nearly 0 to 70, because the state components vary due to the state coupling induced by the electric field. The anisotropic factor decreases from 170 000 to nearly 1 rapidly as the electric field increases. The Zeeman splittings of the electron ground states are always isotropic as the spin-orbit coupling is neglectable in these states.

ACKNOWLEDGMENTS

J.-B. X. and S.-S. L. would like to acknowledge the support from the National Natural Science Foundation of China (No. 90301007 and No. 60521001), and W.-J. F. would like to acknowledge the support from A*STAR (Grant No. 0621200015) and AcRF RGM 1/07.

¹H. Ohno, *Science* **281**, 951 (1998).

²T. Dietl, H. Ohno, F. Matsukura, J. Cibert, and D. Ferrand, *Science* **287**, 1019 (2000).

³T. Dietl, H. Ohno, and F. Matsukura, *Phys. Rev. B* **63**, 195205 (2001).

⁴A. Wall, A. Franciosi, D. W. Niles, R. Reifenberger, C. Quaresima, M. Capozzi, and P. Perfetti, *Phys. Rev. B* **41**, 5969 (1990).

⁵T. Andrearczyk, J. Jaroszyński, G. Grabecki, T. Dietl, T. Fuku-

mura, and M. Kawasaki, *Phys. Rev. B* **72**, 121309(R) (2005).

⁶I. P. Smorchkova, N. Samarth, J. M. Kikkawa, and D. D. Awschalom, *Phys. Rev. Lett.* **78**, 3571 (1997).

⁷A. Waag, Th. Gruber, G. Reuscher, R. Fiederling, W. Ossau, G. Schmidt, and L. W. Molenkamp, *J. Supercond.* **14**, 291 (2001).

⁸C. J. Barrelet, A. B. Greytak, and C. M. Lieber, *Nano Lett.* **4**, 1981 (2004).

⁹H. G. Lee, H. C. Jeon, T. W. Kang, and T. W. Kim, *Appl. Phys. Lett.* **78**, 3319 (2001).

- ¹⁰S. V. Zaitsev-Zotov, Yu. A. Kumzerov, Yu. A. Firsov, and P. Monceau, *J. Phys.: Condens. Matter* **12**, L303 (2000).
- ¹¹S. Banerjee, A. Dan, and D. Chakravorty, *J. Mater. Sci.* **37**, 4261 (2002).
- ¹²J. B. Xia and X. W. Zhang, *Eur. Phys. J. B* **49**, 415 (2006).
- ¹³X. W. Zhang and J. B. Xia, *J. Phys.: Condens. Matter* **18**, 3107 (2006).
- ¹⁴L. Chen, P. J. Klar, W. Heimbrot, F. Brieler, and M. Froba, *Appl. Phys. Lett.* **76**, 3531 (2000).
- ¹⁵C. Cheng, G. Xu, H. Zhang, H. Wang, J. Cao, and H. Ji, *Mater. Chem. Phys.* **97**, 448 (2006).
- ¹⁶C. W. Na, D. S. Han, D. S. Kim, Y. J. Kang, J. Y. Lee, J. Park, D. K. Oh, K. S. Kim, and D. Kim, *J. Phys. Chem. B* **110**, 6699 (2006).
- ¹⁷S.-E. Han, H. Oh, J.-J. Kim, H.-K. Seong, and H.-J. Choi, *Appl. Phys. Lett.* **87**, 062102 (2005).
- ¹⁸P. V. Radovanovic, C. J. Barrelet, S. Gradecak, F. Qian, and C. M. Lieber, *Nano Lett.* **5**, 1407 (2005).
- ¹⁹Y.-H. Zhu and J.-B. Xia, *Phys. Rev. B* **75**, 205113 (2007).
- ²⁰H. W. van Kesteren, E. C. Cosman, W. A. J. A. van der Poel, and C. T. Foxon, *Phys. Rev. B* **41**, 5283 (1990).
- ²¹R. Danneau, O. Klochan, W. R. Clarke, L. H. Ho, A. P. Micolich, M. Y. Simmons, A. R. Hamilton, M. Pepper, D. A. Ritchie, and U. Zuilicke, *Phys. Rev. Lett.* **97**, 026403 (2006).
- ²²R. Danneau, O. Klochan, W. R. Clarke, L. H. Ho, A. P. Micolich, M. Y. Simmons, A. R. Hamilton, M. Pepper, D. A. Ritchie, and U. Zuilicke, *AIP Conf. Proc.* **893**, 699 (2007).
- ²³J.-B. Xia and J. Li, *Phys. Rev. B* **60**, 11540 (1999).
- ²⁴X. W. Zhang and J. B. Xia, *Phys. Rev. B* **72**, 205314 (2005).
- ²⁵J. K. Furdyna, *J. Appl. Phys.* **64**, R29 (1988).